

# Resonant Raman imaging of MoS<sub>2</sub>-substrate interaction

Hongyuan Li<sup>1,2</sup> and Dmitri V. Voronine<sup>1,3</sup>

<sup>1</sup>*Institute for Quantum Science and Engineering,  
Texas A&M University, College Station, TX, 77843 USA*

<sup>2</sup>*Department of Applied Physics, School of Science,  
Xi'an Jiaotong University, Shaanxi 710049, P. R. China*

<sup>3</sup>*Baylor University, Waco, TX, 76798 USA*

## Abstract

We report a study of long-range MoS<sub>2</sub> -substrate interaction using resonant Raman imaging. We observed a strong thickness-dependent peak shift of a Raman-forbidden mode that can be used as a new method of determining the thickness of multilayered MoS<sub>2</sub> flakes. In addition, dependence of the Raman scattering intensity on thickness is explained by the interference enhancement theory. Finally, the resonant Raman spectra on different substrates are analysed.

**Keywords:** MoS<sub>2</sub>, resonant Raman, AFM, thickness-dependence, forbidden mode

## I. INTRODUCTION

Two-dimensional (2D) transition metal dichalcogenide (TMD) materials have recently attracted wide attention due to their potential applications in optoelectronic devices. For example, monolayer MoS<sub>2</sub> has a large direct band gap [1], and can be used in field-effect-transistors[2]. As a powerful tool, Raman spectroscopy has been widely used for studying the various properties of MoS<sub>2</sub>. Frey *et.al.* studied the resonant Raman (RR) spectra of MoS<sub>2</sub> nanoparticles [3]. Li and Chakraborty have investigated the thickness-dependent effects for the Raman scattering of MoS<sub>2</sub> [4, 5]. Also, the influence of the substrate-MoS<sub>2</sub> interactions on the Raman spectra has been investigated [6]. In this paper, we performed RR imaging of multilayered MoS<sub>2</sub> flakes using 660 nm laser excitation which corresponds to the A exciton of MoS<sub>2</sub> [7, 8]. We obtained simultaneously the topographic information and correlated it with Raman imaging. The correlated AFM-Raman imaging reveals the relation between the thickness and optical properties. We also analysed the influence of substrates with different dielectric properties on the RR spectra of MoS<sub>2</sub>.

## II. RESULTS

The multilayered MoS<sub>2</sub> flakes were exfoliated on SiO<sub>2</sub> and gold substrate using the scotch-tape method. The AFM image of a typical MoS<sub>2</sub> flake is shown in Fig.1 (a). The thinnest part of the flake has the height of  $\sim 3\text{nm}$ , which corresponds to 5 layers of MoS<sub>2</sub> [4]. Note the colorbar in Fig.1 (a) corresponds to the number of layers.

A typical RR spectrum of the MoS<sub>2</sub> flake is shown in Fig.1 (b). The main spectral features include: strong out-of-plane A<sub>1g</sub> mode near  $410\text{cm}^{-1}$ , in-plane E<sub>2g</sub><sup>1</sup> mode near  $385\text{cm}^{-1}$ , IR-active A<sub>2u</sub> mode near  $466\text{cm}^{-1}$  and several second-order modes, which include E<sub>1g</sub>+LA at  $528\text{cm}^{-1}$ , 2E<sub>1g</sub> at  $574\text{cm}^{-1}$ , E<sub>2g</sub><sup>1</sup>+LA at  $600\text{cm}^{-1}$  and A<sub>1g</sub>+LA at  $644\text{cm}^{-1}$  [3, 4].

Resonant Raman imaging of the multilayered MoS<sub>2</sub> flake on the gold substrate is shown in Fig.2. The imaging step size was 100nm. The intensity maps for A<sub>1g</sub> and A<sub>2u</sub> modes are shown in Fig.2 (a) and (b). The intensity ratio I(A<sub>2u</sub>)/I(A<sub>1g</sub>) is shown in Fig.2 (c). Both Fig.2 (a) and (b) show that the area with the strongest intensity corresponds to the number of layers of about 30, while the very thin (eg: the middle) and the very thick (eg: the left bottom) parts of the flake show a relatively low intensity. I(A<sub>1g</sub>) vs the number of layers is shown in Fig.4 (b) where the maximum intensity correspond to n=30. The intensity ratios in Fig.4 (a) and Fig.5 indicate that

for the thin part, the  $A_{2u}$  peak has a relatively stronger intensity compared to other modes.

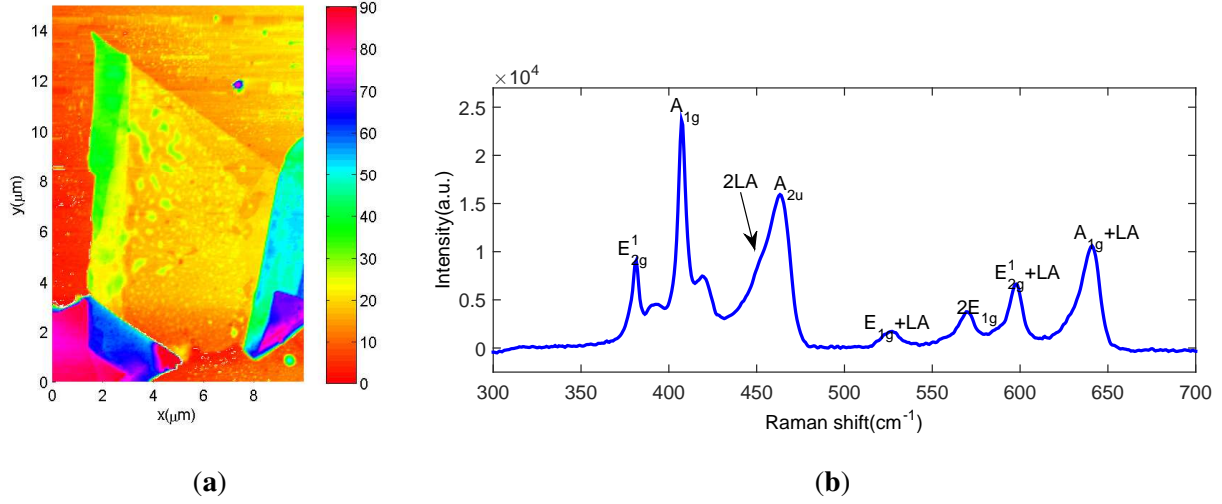


FIG. 1. AFM image (a) of MoS<sub>2</sub> flake, with the colorbar representing the number of layers and a typical resonant Raman spectrum (b) of a multilayered MoS<sub>2</sub> flake on gold substrate excited by 660 nm laser.

Peak positions also show shifts with the change of the number of layers. The peak position maps of the  $A_{1g}$  and  $A_{2u}$  modes are shown in Fig.2 (d) and (e). Combined with the height distribution in Fig.1 (a), the RR spectra show a blue shift for  $A_{1g}$  and a red shift for  $A_{2u}$  for a multilayered flake compared to bulk MoS<sub>2</sub>. Fig.3 (a) and (b) show the  $A_{1g}$  and  $A_{2u}$  peak position versus the number of layers. The  $A_{1g}$  peak position increases slightly ( $\sim 0.5 \text{ cm}^{-1}$ ) when the number of layers increases from 7 to 140, while the  $A_{2u}$  peak has a blue shift of about  $\sim 2 \text{ cm}^{-1}$ . The shift of the  $A_{2u}$  peak can be seen more clearly in Fig.5 (a) and (b).

### III. DISCUSSION

We consider two main effects: (1) substrate dependence, (2) thickness-dependence, including peak shifts and intensity variations. It has been widely reported that, on common insulating substrates such as silicone and SiO<sub>2</sub>, the increase of the number of layers has an influence on the two characteristic Raman peaks  $E_{2g}^1$  and  $A_{1g}$  [4, 9]. The  $A_{1g}$  mode has a blue shift due to the increase of the force constant which is induced by the increased interlayer van der Waals interaction. Our RR measurements of the  $A_{1g}$  peak position variation are consistent with the previous reports. However, here we show that, under the resonant condition, the Raman-inactive  $A_{2u}$  mode shows a strong thickness-dependent softening with the increase of the number of layers. This is attributed

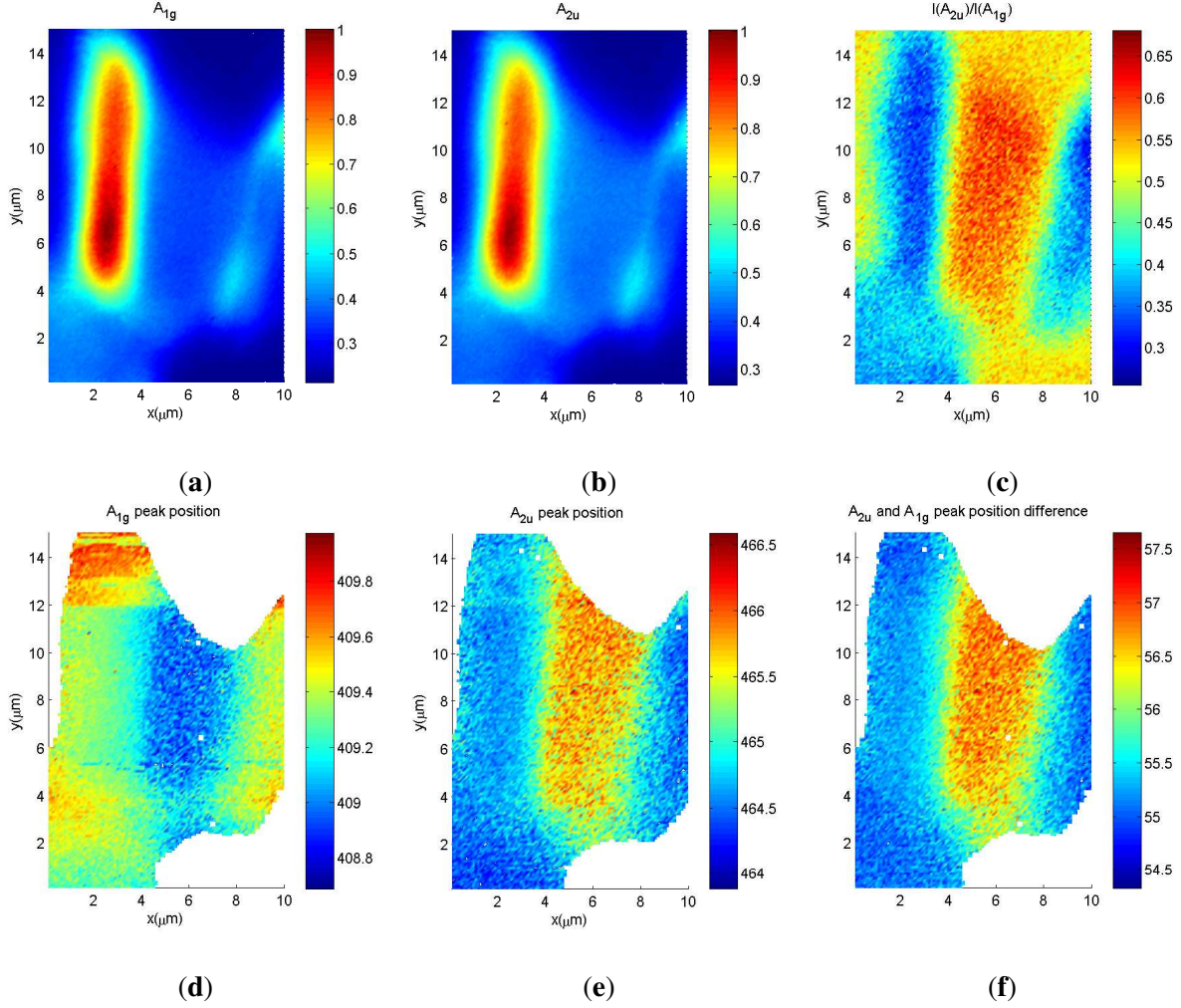


FIG. 2. Resonant Raman imaging of multilayered MoS<sub>2</sub> on gold substrate: intensity of A<sub>1g</sub> (a) and A<sub>2u</sub> (b) modes, peak intensity ratio  $I(A_{2u})/I(A_{1g})$  (c), peak portion maps for A<sub>1g</sub> (d) and A<sub>2u</sub> (e) modes, and peak position difference A<sub>2u</sub>-A<sub>1g</sub> (f).

to the decrease of the long-range Coulombic interaction between the Mo atoms with increasing layer number [10]. The results on SiO<sub>2</sub> substrate are consistent with previous reports. For the small number of layers ( $n < 10$ ), the thickness-dependent RR signal of both A<sub>1g</sub> and A<sub>2u</sub> mode show red shifts with the increase of the number of layers [4]. When the number of layers exceeds  $\sim 10$ , the change of the peak position is small and difficult to measure.

However on the gold substrate, we observed a previously unreported blue shift for the A<sub>2u</sub> mode. Fig.3 (a) shows that for a small number of layers ( $\sim 6$ ), the A<sub>2u</sub> peak has a red shift of about  $2\text{cm}^{-1}$  compared to the bulk MoS<sub>2</sub>. With the increase of the thickness, this red shift gradually disappears with a turning point near  $n = 30$ , as shown in Fig.3 (a). This indicates that

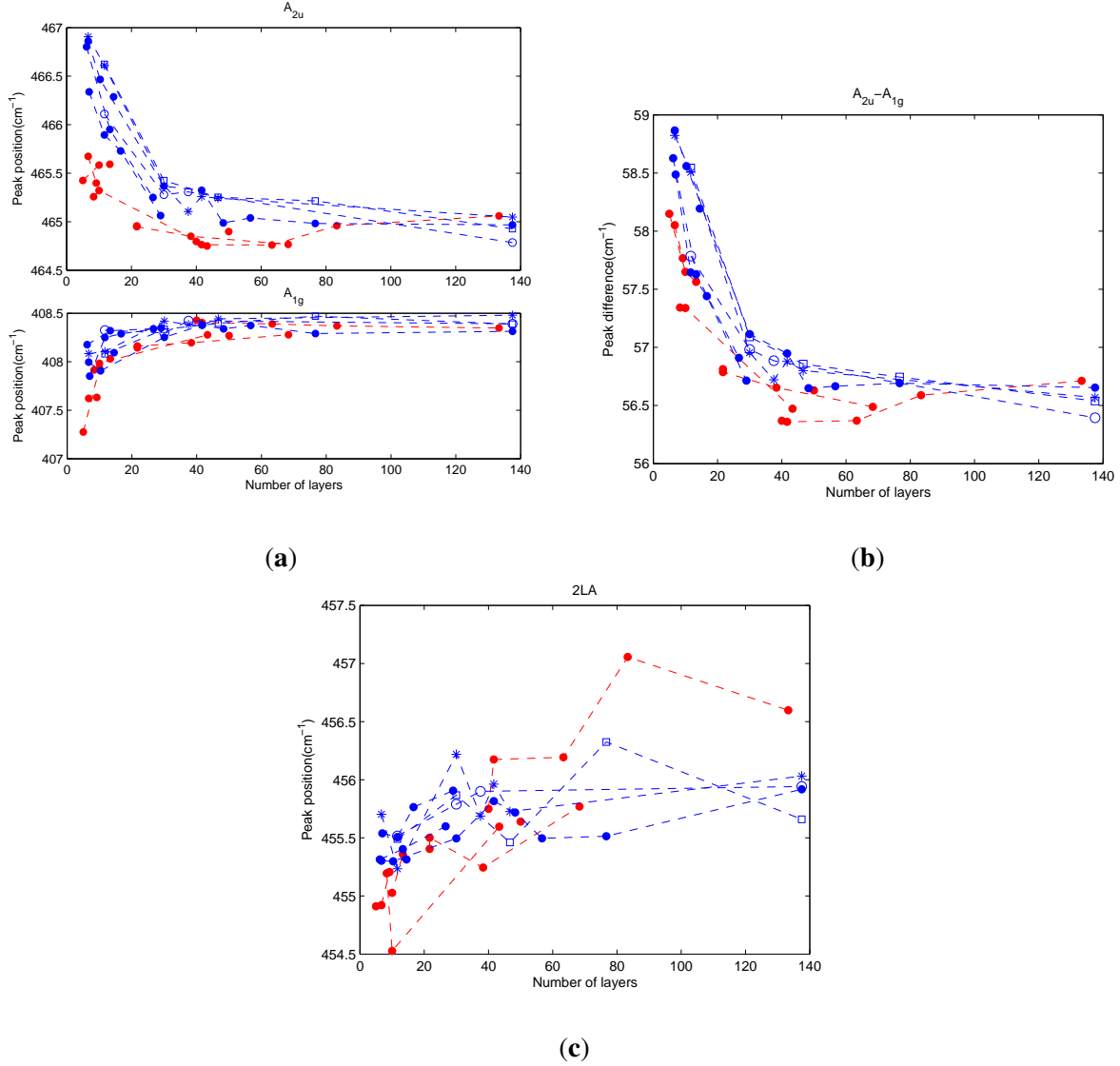


FIG. 3. Thickness-dependence of peak position. **(a)** Peak position of  $A_{2u}$  and  $A_{1g}$  modes. **(b)** Peak position difference  $A_{2u}-A_{1g}$ . **(c)** Peak position of 2LA. Blue and red dots represent the measurements on gold and SiO<sub>2</sub> substrates, respectively. Data from several flakes are shown as groups of points linked by dashed lines with all connected points belonging to the same flake

the thickness-dependent effects can be observed within a large range of the number of layers. This is different from the SiO<sub>2</sub> substrate where the peak shift can only be observed for a small number of layers ( $n < 10$ ).

We consider two possible reasons for the different peak shift directions of the  $A_{2u}$  mode of the multilayered MoS<sub>2</sub> flake on the gold substrate: (1) laser-induced heating of the gold substrate may have thermal effects on MoS<sub>2</sub> leading to the peak shift [11]; (2) charge transfer from MoS<sub>2</sub>

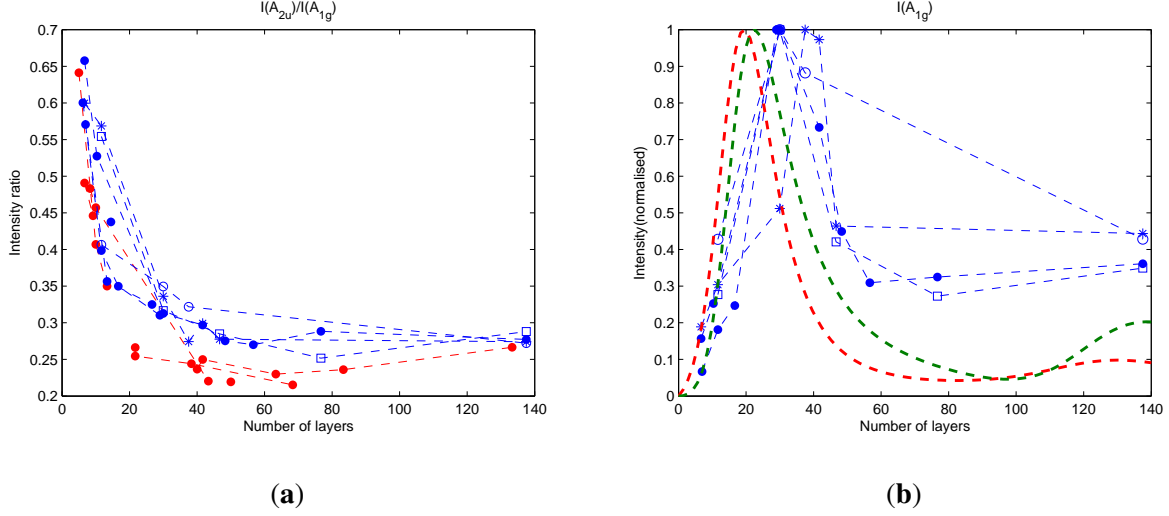


FIG. 4. (a). The intensity ratio  $I(A_{2u})/I(A_{1g})$  decreases rapidly with the increase of the thickness and stabilizes after a turning point of  $\sim 10$  nm. (b)  $A_{1g}$  intensity as a function of thickness shows a maximum at  $\sim 30$  layers. Red dashed line shows the simulation

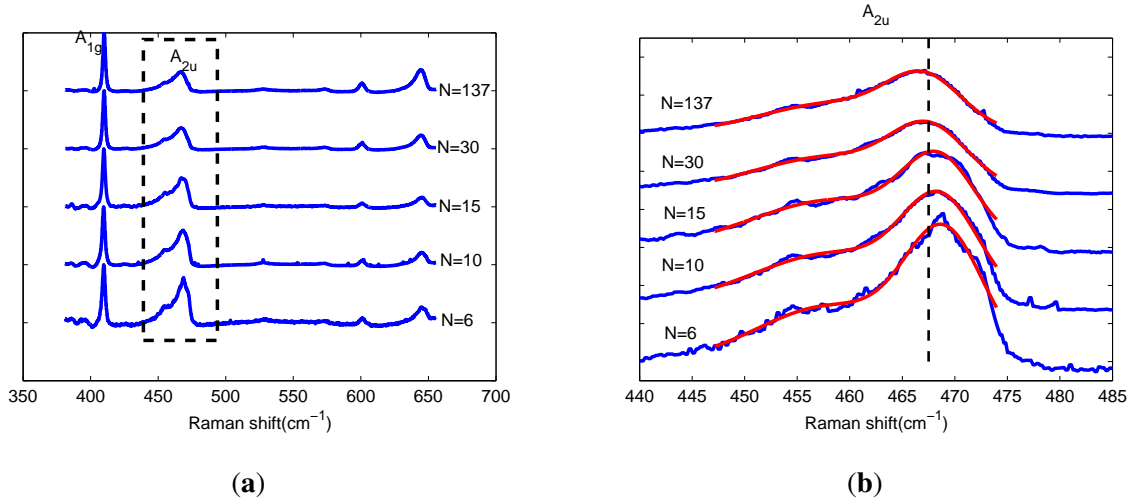


FIG. 5. (a) Resonant Raman spectra for different number of layers  $N$  (normalised to  $A_{1g}$  and offset for convenience). (b) Spectra of the  $A_{2u}$  mode, corresponding to the dashed spectral region in (a).

to the gold substrate modifying the doping, and the electron-phonon interactions [6, 12]. We discard the first possibility by performing laser power dependent measurements. Different laser power can lead to different surface temperatures. However, we find no observable changes in the peak position vs the number of layers for different laser powers (Fig.3). The second possible explanation may be supported by previous literature reports which considered the non-resonant situation. Several studies reported p-doping of MoS<sub>2</sub> using various methods, including deposition on the gold substrate [6, 13], decoration with gold nano-particles (NP) [14], and using monolayer

MoS<sub>2</sub> transistor to adjust the doping level directly [15] resulting in stiffening of the A<sub>1g</sub> mode. Here our results show the corresponding blue shift of the A<sub>1g</sub> mode on the gold substrate for the number of layers N<10, which is consistent with the previous studies. Here, we, for the first time, observed that under the resonant conditions, the Raman-inactive A<sub>2u</sub> mode of MoS<sub>2</sub> on the gold substrate shows a strong blue shift compared with that on the SiO<sub>2</sub> substrate. Fig.3 (a) shows a shift more than 1cm<sup>-1</sup> when the number of layers is less than 10 layers.

Fig.4 shows the nearly linear increase of the A<sub>1g</sub> peak intensity until the number of layers reaches ~30 with the maximum point n=30, followed by a decrease until n=50. Note that the Raman signal intensity of bulk MoS<sub>2</sub> is weaker than that with the number of layers of ~30. This may be attributed to the inference enhancement[16, 17] due to multiple reflections of the incident laser and emitted Raman signals in MoS<sub>2</sub> flakes. Using the model of Wang *et.al.*, the intensity of the Raman signal can be expressed as

$$I = \int_0^d |t\gamma|^2 dy, \quad (1)$$

where  $d$  is the thickness of the MoS<sub>2</sub> flake,  $t$  is the amplitude of the electric field at the depth  $y$ , and  $\gamma$  is the enhancement factor due to the multiple-reflection. The simulation is shown as a red dashed line in Fig.3 (b). The original model assumes no coherence between the field scattered from adjacent layers. Considering coherence, Eq. (1) can be written as

$$I = \left| \int_0^d t\gamma dy \right|^2. \quad (2)$$

The coherent simulation is different, shown as a green dashed line in Fig.3 (b). Zeng *et.al.* provided a qualitative explanation by using the accumulated phase shift for the  $n_{th}$  reflected field and destructive interference with the first reflected field from the flake surface [18].

## ACKNOWLEDGEMENTS

We thank Profs. Marlan Scully, Alexei Sokolov and Zhenrong Zhang for helpful discussions. We also thank Prof. Marlan Scully for the access to Raman facilities and we thank Zhenrong Zhang for help with sample preparation. D.V. acknowledges the support of NSF grant CHE-1609608.

---

[1] A. Splendiani, L. Sun, Y. B. Zhang, T. S. Li, J. Kim, C. Y. Chim, G. Galli, and F. Wang, Nano Lett. **10**, 1271 (2010).

- [2] J. Lin, H. Li, H. Zhang, and W. Chen, Appl. Phys. Lett. **102**, 203109 (2013).
- [3] G. L. Frey, R. Tenne, M. J. Matthews, M. Dresselhaus, and G. Dresselhaus, Physical Review B **60**, 2883 (1999).
- [4] B. Chakraborty, H. S. S. R. Matte, A. K. Sood, and C. N. R. Rao, J. Raman Spectrosc. **44**, 92 (2013).
- [5] H. Li, Q. Zhang, C. C. R. Yap, B. K. Tay, T. H. T. Edwin, A. Olivier, and D. Baillargeat, Advanced Functional Materials **22**, 1385 (2012).
- [6] M. Buscema, G. A. Steele, H. S. J. van der Zant, and A. Castellanos-Gomez, Nano Res. **7**, 561 (2014).
- [7] R. Coehoorn, C. Hass, and R. A. de Groot, Phys. Rev. B **35**, 6023 (1987).
- [8] J. V. Acrivos, W. Y. Liang, J. A. Wilson, and A. D. Yoffe, J. Phy. C **4**, L18 (1971).
- [9] H. Li, Q. Zhang, C. C. R. Yap, B. K. Tay, T. H. T. Edwin, A. Olivier, and D. Baillargeat, Adv. Funct. Mater. **22**, 1385 (2012).
- [10] A. M. Sanchez and L. Wirtz, Phys. Rev. B **84**, 155413 (2011).
- [11] S. Najmaei, A. Mlayah, A. Arbouet, C. Girard, J. Leotin, and J. Lou, NANO **8**, 12682 (2014).
- [12] U. Bhanu, M. R. Islam, L. Tetard, and S. I. Khondaker, Sci. Rep. **4**, 5574 (2014).
- [13] B. J. Robinson, C. E. Giusca, Y. T. Gonzalez, N. D. Kay, O. Kazakova, and O. V. Kolosov, 2D Materials **2**, 015005 (2015).
- [14] Y. Shi, J. Huang, L. Jin, Y. Hsu, S. Yu, L. Li, and H. Yang, Scientific Reports **3**, 1839 (2013).
- [15] B. Chakraborty, A. Bera, D. Muthu, S. Bhowmick, U. V. Waghmare, and A. Sood, Phys. Rev. B **85**, 161403 (2012).
- [16] Y. Y. Wang, Z. H. Ni, Z. X. Shen, H. M. Wang, , and Y. H. Wu, Appl. Phys. Lett. **92**, 043121 (2008).
- [17] Z. Ni, Y. Wang, T. Yu, and Z. Shen, Nano Res **1**, 273 (2008).
- [18] J. Zeng, J. Li, H. Li, Q. Dai, S. Tie, and S. Lan, Optics Express **23**, 31817 (2015).